Carbohydrate Polymers 94 (2013) 137–146

Contents lists available at SciVerse ScienceDirect

Carbohydrate Polymers

journal homepage: www.elsevier.com/locate/carbpol

The effect of poly-L-lysine structure on the pH response of polygalacturonic acid-based multilayers

Marta Westwood, Timothy R. Noel, Roger Parker*

Institute of Food Research, Norwich Research Park, Colney, Norwich NR4 7UA, United Kingdom

ARTICLE INFO

Article history:
Received 13 September 2012
Received in revised form
18 December 2012
Accepted 26 December 2012
Available online 3 January 2013

Keywords:
Polysaccharide
Polyamino acid
Dendrimer
Disassembly
Dual polarisation interferometer
Multilayer

ABSTRACT

The effect of poly-L-lysine (PLL) molecular weight and structure on pH stability of polygalacturonic acid (PGaLA)-based multilayer films is studied over a pH cycle 7.0–1.6–7.0. The multilayer assembled with the lowest molecular weight PLL (1 kDa) showed the largest pH response. Only 12% of the mass remained and a preferential loss of PLL was observed. Extensive structural reorganisation of the layer as the pH was increased was due to the PGaLA reionisation leading to extensive net loss of hydrated mass. The multilayers assembled with the higher molecular weight linear PLLs (10 kDa, 200 kDa) showed loss of about 50% of their initial polymer mass. The multilayer assembled with the dendrimer (22 kDa) showed a stronger response to pH compared to the linear higher molecular weight PLLs. Over the pH cycle a loss of about 60% polymer mass and a decrease in the film thickness was observed. Despite having a reduced density at pH 1.6, the density substantially recovered to 0.54 g mL^{-1} on return to pH 7.0.

1. Introduction

Layer by layer deposition techniques offer a versatile means of engineering interfacial polymer films with diverse properties. Whereas the majority of studies employ synthetic polyelectrolytes (Decher, 1997) the use of the technique to assemble films and coatings from naturally occurring biopolymers and, more specifically, charged polysaccharides is also becoming well established (Boudou, Crouzier, Ren, Blin, & Picart, 2010; Crouzier, Boudou, & Picart, 2010). The films can be used in the fabrication of nanostructured dispersed systems such as microcapsules with multiple functionalities (Pommersheim, Schrezenmeir, & Vogt, 1994; Sukhorukov & Mohwald, 2007). Applied to emulsion systems multilayers can enhance stability (Guzey & McClements, 2006), and modulate their digestibility in the human gastrointestinal tract and affect the release of lipophilic components (Li et al., 2010; McClements & Li, 2010). Recent studies of carbohydrate polymer-based multilayer films have found that the rules governing their growth and functional behaviour are different from those for synthetic polymer-based multilayer films. For example, polyamino acid–anionic polysaccharide multilayers (Crouzier & Picart, 2009) grow with constant ratios of polyamino acid-monosaccharide repeating groups rather than intrinsic charge balance determining the stoichiometry. The relationship between polysaccharide structure, polysaccharide multilayer assembly and properties remains incompletely understood.

The aim of the present study is to examine the effect of polycation molecular weight and branching on the growth and pH-responsiveness of polygalacturonic acid-based multilayer films. Poly-L-lysine (PLL), a polyamino acid, was chosen because it is highly charged and also commonly used, allowing comparison with other studies including our own previous work (Krzeminski et al., 2006; Moffat, Noel, Parker, Wellner, & Ring, 2007). Its cationic charge at neutral and acidic pH's derives from its side chains which each carry a weakly basic ε-amino group with pK_a about 9 (Girod et al., 2004). Our previous work was limited to a single relatively low molecular weight linear polycation (Westwood, Noel, & Parker, 2011). In this study both an oligomeric and high molecular weight polycation and a branched PLL dendrimer are included. The polyanion chosen for multilayers assembly was polygalacturonic acid (PGaLA), a highly-charged cell wall polysaccharide (Alberts et al., 2002), more specifically a deesterified pectin which is typically extracted from the peel of citrus fruit. PGaLA is a weak polyelectrolyte based on a backbone of (1–4)-α-galacturonysyl units. In pectin, PGaLA backbone is interrupted in places by (1–2)-α-L-rhamnopyranosyl units (Cros, Garnier, Axelos, Imberty, & Perez, 1996). The pK_a of anhydrogalacturonic acid residues in PGaLA are in the range 3.0–4.5 (Ralet, Dronnet, Buchholt, & Thibault, 2001) and the polymer has a persistence length of 10–12 nm and is thus classified as semi-flexible (Cros et al., 1996).

* Corresponding author. Tel.: +44 01603 255000; fax: +44 01603 507723.
E-mail address: roger.parker@ifr.ac.uk (R. Parker).

0144-8617/$ – see front matter © 2013 Elsevier Ltd. All rights reserved.
http://dx.doi.org/10.1016/j.carbpol.2012.12.065

A basic property of multilayers assembled from weakly acidic polysaccharides and weakly basic polyamino acids is their pH-responsive behaviour. Responses reported range from conformational changes of polyamino acids (Zhi & Haynie, 2004) to swelling (Burke & Barrett, 2003), partial dissolution (Boulmedais, Bozonnet, Schwinte, Voegel, & Schaaf, 2003), dissolution of a sacrificial layer (Ono & Decher, 2006) and complete dissolution of the multilayer film (Boulmedais et al., 2003). These pH responses can be coupled to release of additional species incorporated into the multilayers. Model systems have been fabricated in which both the rate and extent of the release of dye tracers loaded into the film depend upon pH (Burke & Barrett, 2004; Hiller & Rubner, 2003). In our own work we have found that highly esterified pectins (degree of esterification, DE71)-poly-L-lysine multilayers show shrinkage and preferential loss of PLL crosslinker as the pH falls from 7.0 to 3.5, i.e. as it approaches the pK_a of the anhydrogalacturonic acid groups of the pectin (Moffat et al., 2007). In this and subsequent work (Westwood et al., 2011) the emphasis was on responses to a pH cycle starting from neutral, falling to acid pH, and returning to neutral pH. These conditions were chosen to mimic those in the human gastrointestinal (GI) tract as one potential application of multilayer films is their use in the modulation of release in the GI tract (Li & Jasti, 2006). Multilayers assembled with the more highly charged PGalA showed shrinkage at lower pH (<3.5) as the pH is reduced from 7.0 and, on increasing the pH after taking the multilayers to pH 1.5, a sharp swelling event occurs at pH 4.0 as the pH increased towards 7.0 (Westwood et al., 2011). FTIR-ATR showed the multilayer composition was far from achieving intrinsic charge balance and the polymers could sustain both net positive (pH 7.0) and net negative (pH 1.5) charges during a responsiveness experiment.

In order to obtain a better understanding of the influence of the molecular weight and the structure of the polycation on the multilayer growth and pH responsiveness, we have chosen linear PLL with molecular weights in the range 1–300 kDa and a 22 kDa PLL dendrimer for our study. Multilayers were prepared on the silicon oxide surfaces and characterised with a dual polarisation interferometer, Fourier transform infrared spectrophotometer and a quartz crystal microbalance to study changes in the optical thickness and polymer concentration, composition, speciation and hydrated mass of the films occurring during their assembly and subsequent experiments on their pH responsiveness.

2. Materials and methods

2.1. Polymers and polymer solution preparation

Linear poly-L-lysine hydrobromide with nominal low, intermediate and high molecular weights, 500–2000 Da (LMW, P8954), 4.0–15.0 kDa (IMW, P6516) and 150.0–300.0 kDa (HMW, P1399) and D_2O (99.9%), respectively, were obtained from Sigma, and polygalacturonic acid (Krzeminski et al., 2006) was supplied by Fluka, Biochemika. A dendrigraft poly-L-lysine (DGL) trifluoroacetate dendrimer (DEN) with molecular weight 22.0 kDa and a hydrodynamic diameter of 7 nm (Cottet et al., 2007) was supplied by Colcom SARL, Montpellier, France. Reagents were analytical grade.

For the multilayer assembly solutions of 0.6 mg mL^{-1} were prepared by dissolving the biopolymers in 10 mM pH 7.0 phosphate buffer, containing 30 mM NaCl which provided both pH control and a background level of ionic strength. The NaCl concentration was chosen to enhance the complexation between the polysaccharide and polyamino acids (Wen & Dubin, 1997). The pH was adjusted by adding 0.1 M NaOH. For pH responsiveness studies the following buffers were prepared: HCl/KCl (pH 1.6–2.9), acetate (pH 3.6–4.8) and phosphate buffers (pH 6.0 and 7.0); each containing 30 mM NaCl.

2.2. Multilayer formation

The multilayer structures were fabricated on a silicon oxide substrate by layer-by-layer deposition (Decher, 1997) at 20 °C, following the procedure, which has been described in detail elsewhere (Krzeminski et al., 2006; Westwood, Noel, & Parker, 2010). Prior to deposition the substrate surfaces were cleaned using a UV-Ozone chamber (Bioforce Nanosciences, Inc., Iowa, USA), then rinsed thoroughly with water and dried with N_2. For all of the multilayer films the base layer was formed by deposition of PLL. The multilayer assembly of PGalA-based films was then subsequently formed by alternate exposure of the PLL-coated substrate to a PGalA solution and then to a PLL solution. All multilayer assemblies studied consisted of a total of 10 layers.

2.3. pH responsiveness studies

To assess the multilayer response to pH, the previously formed 10-layer films were first exposed to solutions of decreasing pH, starting from 7.0 down to 1.6. In order to study the reversibility of the process and broadly mimic the pH change in the gastrointestinal tract the pH was then increased in the same steps back to 7.0. At each step the buffer solutions were left in contact with the films for sufficient time to collect data of suitable accuracy. The QCMD measurements were made in real time over a 5 min period after the introduction of each buffer solution. The DPI measurements were made whilst flowing the buffer solutions over the samples for 5 min. For the FTIR-ATR the buffer was injected into the measurement cell and the spectra were recorded by co-adding 512 scans in the frequency range 1500–1800 cm^{-1} with a resolution of 2 cm^{-1} over an 8 min period and subtracting a buffer background. After responsiveness studies surfaces were cleaned with 2% (v/v) Hellmanex, rinsed with water, exposed to UV-Ozone treatment, and then rinsed with water again. Surfaces were dried with N_2.

2.4. Quartz crystal microbalance with dissipation monitoring (QCMD)

The multilayer assembly and pH responsiveness were monitored using a D300 QCMD (Q-Sense AB, Västra Frölunda, Sweden) with a QAFC 302 axial flow measurement chamber as described elsewhere (Krzeminski et al., 2006; Westwood et al., 2010). Silicon dioxide coated AT-cut quartz crystals sandwiched between gold electrodes (QSX-303, Q-Sense AB, Västra Frölunda, Sweden) were used as the substrate. This QCMD sensor was placed in the measurement chamber and an AC voltage was applied to excite the fundamental resonant frequency (~5 MHz) of the crystal and its overtones (3rd, 5th and 7th). Each layer was formed during a 4 min exposure of the sensor surface to a biopolymer solution, and each deposition step was followed by a buffer rinse. The assembly and environmental response studies were carried out in real-time by monitoring changes in the oscillation frequency of the crystal. The responsiveness measurements were made as described above. A decrease in oscillation frequency indicates the adsorption of mass onto the QCMD sensor. If the mass is deposited evenly and forms a rigid elastic layer, then the negative frequency changes are proportional to the hydrated mass deposited (Δm) as described by the Sauerbrey equation (Sauerbrey, 1959)

$$\Delta m = \frac{-C\Delta f_n}{n} \quad (1)$$

where C is the mass sensitivity constant (C = 17.7 ng cm^{-2} Hz^{-1} for a 5 MHz crystal (Hook et al., 2001)) and Δf_n the frequency shift of the nth overtone. For viscoelastic materials, the Sauerbrey relation leads to an underestimate of the deposited hydrated mass and, under these conditions, a more detailed analysis was

performed using the Voigt model (Voinova, Rodahl, Jonson, & Kasemo, 1999) with the QTools™ modelling package (Q-Sense AB, Västra Frölunda, Sweden).

2.5. Dual polarisation interferometry (DPI).

The measurements were carried out using an AnaLight Bio200 DPI (Farfield Scientific, Crewe, UK) with a silicon oxynitride sensor chip (Halthur, Claesson, & Elofsson, 2006; Lu, Swann, Peel, & Freeman, 2004). The sensor chip consists of a sandwich of two horizontally stacked waveguides, a sensing waveguide on top of a reference waveguide separated by an opaque cladding material. Laser light (wavelength, 632.8 nm) illuminating one end of the chip is switched between two polarisations: transverse magnetic (T_M) and transverse electric (T_E); the light travels along the waveguides and on exiting the chip produces an interference fringe pattern, which is detected by a camera located at the far field. A gasket on top of the sensing waveguide forms two measurement chambers, each 1 mm wide, 17 mm long and 1 mm deep (volume 17 μL). The principle of DPI measurement is that changes in the refractive index and thickness of an adsorbed layer on the sensing waveguide surface cause a phase change in the light travelling down the waveguide and, ultimately, a shift in the interference patterns detected by the camera which differ for vertically and horizontally polarised light. In order to extract structural information from these two phase changes, the simplest assumption made is that the adsorbed film behaves as a single homogeneous layer of uniform refractive index (RI), n_f, and thickness, d_f. By solving Maxwell's equations simultaneously for the two polarisations, unique values for the mean refractive index and optical thickness of the adsorbed film are obtained.

At the start of each experiment the sensing chip was calibrated with 40% (w/w) ethanol and water. Multilayers were assembled by injecting 100 μL of biopolymer solution into a continuously flowing buffer (flow rate, 20 μL min^{-1}) using an HPLC sampling valve. After each injection there was a rinsing step of 5 min. Once the multilayers were assembled the responsiveness measurements were made as described above.

The De Feijter equation (De Feijter, Benjamins, & Veer, 1978) was used to quantify the adsorbed mass, Γ, from the mean optical adsorbed film thickness, d_f, the refractive index of the film, n_f, and dn/dc, the refractive index increment of solutions of the constituent polymers

$$\Gamma = d_f \frac{n_f - n_{buffer}}{dn/dc} \quad (2)$$

where n_{buffer} is the RI of the buffer. dn/dc was assumed to take a value of 0.15 which is typical value of the range of values for polysaccharides and polyamino acids.

2.6. Fourier transform infrared spectroscopy with attenuated total reflection mode (FTIR-ATR)

Spectra were collected on a Nicolet Magna 860 FTIR spectrometer (Thermo Electron Corporation, Madison, USA) fitted with the MicroCircle liquid ATR cell (SpectraTech, Warrington, UK) with a silicon rod ATR crystal (Thermo Electron Corporation, Madison, USA) which presents a silicon oxide surface. All solutions were prepared in D_2O-based phosphate buffer in order to eliminate the stretching mode associated with OH groups which overlap with the amide I band. The multilayer deposition has been fully described elsewhere (Westwood et al., 2010). In brief, 1.0 mL of each biopolymer solution was injected into the measurement cell and was left for 4 min prior to rinsing with 2.0 mL of deuterated buffer. In order to characterise the assembly process spectra were collected over a 16 min period prior to the injection of the next biopolymer solution. Once assembled the responsiveness measurements were made as described above.

3. Results and discussion

3.1. Assembly of PGalA-PLL multilayers at pH 7.0

PGalA-PLL multilayers were assembled on silicon oxide substrates to study the effect of PLL molecular weight and structure on multilayer growth and pH responsiveness. These studies were performed with DPI, FTIR and QCMD techniques which provided complementary information on changes in the hydrated mass, polymer mass, thickness, density, composition and speciation within the multilayers both during their assembly and subsequent experiments on the pH responsiveness of these multilayer structures.

Fig. 1A and B shows the changes in the optical thickness and polymer mass during the assembly of PGalA-based multilayer films. The growth of thickness and mass shows exponential dependence for all the PLLs studied. The rate of multilayer growth increases with increasing molecular weight for the linear PLLs, which is consistent with the earlier studies of Kujawa et al. (Kujawa, Moraille, Sanchez, Badia & Winnik, 2005) and Porcel et al. (Porcel, Lavalle, Decher, Senger, Voegel & Schaaf, 2007). The quantitative parameters describing the assembled 10-layer films are summarised in Table 1. These show that the optical thickness increases from 8 nm to 37 nm as the linear PLLs range from LMW to HMW. The PGalA-PLL dendrimer multilayer has the highest growth rate despite its molecular weight of 22 kDa which is of the same order as the intermediate molecular weight PLL, IMW, used in this study. The dendrimer multilayer with a final thickness of 94.9 nm is about 2.5 times greater than that of the HMW PLL multilayer indicating that the dendrimer is an effective crosslinker. This suggests that the dendrimer structure plays an important role in the assembly of the multilayer films. While linear polymers can adopt extended conformations and lie relatively flat upon a surface the branching of the dendrimer constrains the molecule to adopt a less extended, more globular conformation when it is adsorbed (Bosman, Janssen & Meijer, 1999). The more globular conformation of the dendrimers will add greater thickness to the growing multilayer and will result in more rapid growth.

The variation of the polymer concentration during multilayer deposition changes qualitatively with PLL molecular weight and structure (Fig. 1C–F). The assembly of multilayers with the lowest molecular weight PLL resulted in initially high polymer concentration of 1.0 g mL^{-1} for the base layer. However, during the multilayer assembly, a significant decrease of the polymer concentration is observed each time a PGalA layer is deposited and as the assembly of 10 layer structure is completed the polymer concentration reaches its final value of 0.52 g mL^{-1}. The polymer concentration of the IMW PLL base layer shows a lower initial value of 0.78 g mL^{-1} compared to the polymer concentration of the LMW base layer.

The polymer concentration of the IMW PLL multilayer also decreases with each deposition of PGalA layer. However, in this case it reaches a constant pattern of concentration change after 6 deposition steps. The polymer concentration of the HMW PLL multilayer commences from a low value of 0.65 g mL^{-1} and shows a continuous decrease over the first four deposition steps before increasing to a final value of 0.78 g mL^{-1} (Fig. 1E). The high molecular weight of the HMW PLL (200 kDa) means that, in contrast to the relatively low molecular weight LMW and IMW PLLs, it has a similar molecular size to the PGalA (Westwood et al., 2010). This suggests that the longer-ranged interactions of the high

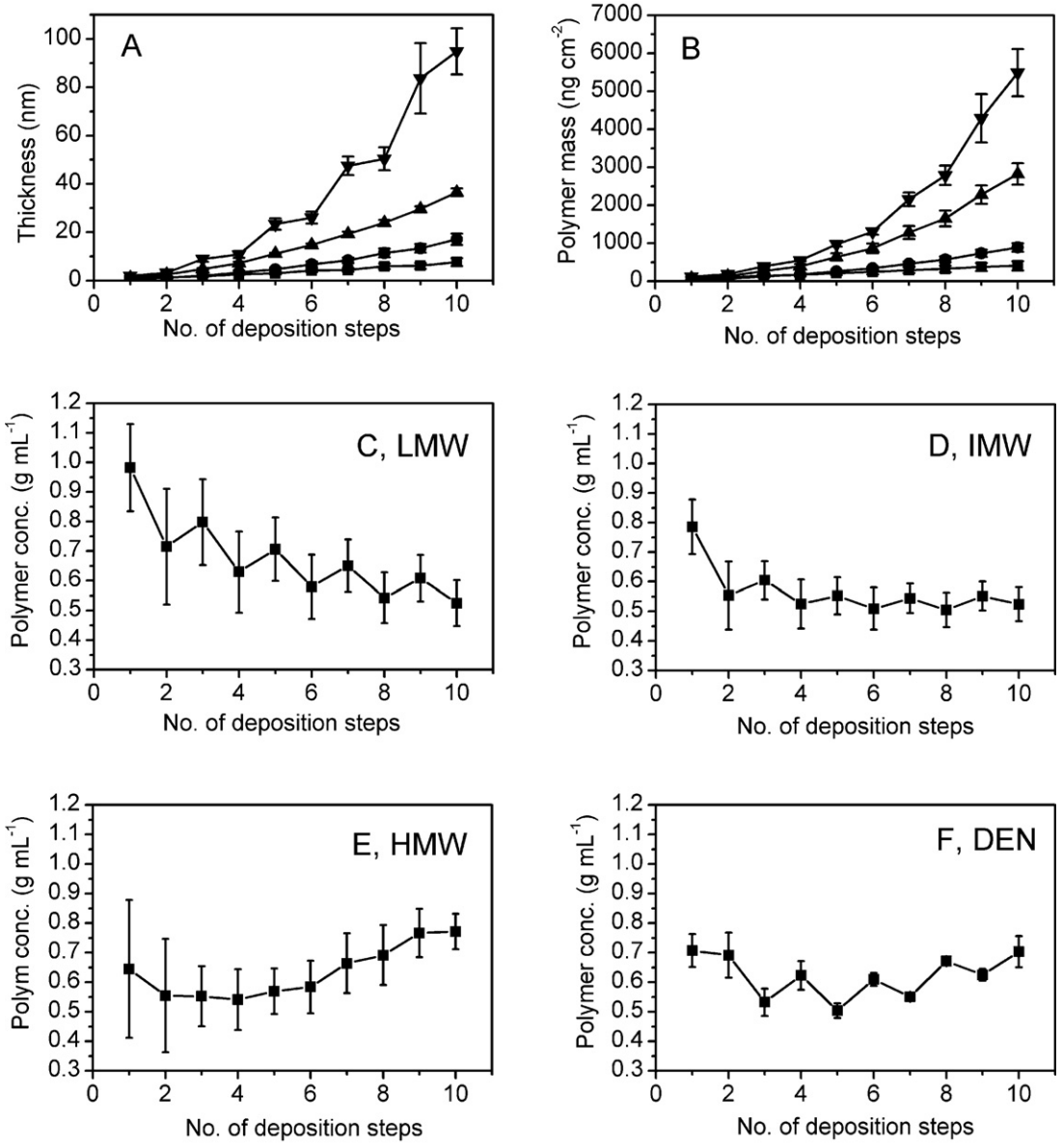

Fig. 1. The assembly of PGalA-PLL multilayer films at pH 7.0 as measured with DPI. The evolution of optical thickness (A), polymer mass (B), and polymer concentration (C–F) are shown as a function of the number of deposition steps. The first deposition step is PLL followed by PGalA, etc. Key to PLLs: LMW (■); IMW (●); HMW (▲); DEN (▼).

molecular weight PLL crosslinker are necessary to obtain a denser, more compact multilayer. Finally, in contrast to the linear PLLs, the polymer concentration of the dendrimer-crosslinked PGalA multilayer increases whenever the PGalA is deposited. This reflects the significant effect of a different structure on the growth of the PGalA-PLL dendrimer multilayer. The highly branched compact dendrimer initially generates a low concentration, more open-structured multilayer, which ultimately, after more deposition and rinsing cycles, increased to a concentration of 0.7 g mL^{-1}. The final refractive index, mass and polymer concentration of the multilayers shown in Table 1 revealed that the HMW PLL leads to the densest multilayer and the PLL dendrimer to the highest mass.

In order to investigate the effect of the molecular weight and the structure of PLL on a formation of the hydrated structure QCMD measurements were performed. Table 1 also shows the frequency shifts and dissipation measured using QCMD for the assembled PGalA-PLL multilayers. The hydrated mass of the multilayers have been calculated from the frequency shift, $\Delta f_3/3$, using the Sauerbrey equation (1). As expected the hydrated mass shows the same trend with molecular weight and structure as is observed using the

Table 1
The effect of PLL molecular mass and structure on the thickness, refractive index, polymer mass and polymer concentration of PGalA-PLL multilayers as measured using dual polarisation interferometry and the frequency shift, Sauerbrey hydrated mass and dissipation measured using a quartz crystal microbalance with dissipation monitoring.

PLL	Thickness (nm)	RI	Polymer mass (ng cm^{-2})	Polymer concentration (g mL^{-1})	$\Delta f_3/3$ (Hz)	Δm_3 (ng cm^{-2})	ΔD_3 ($\times 10^{-6}$)
LMW	7.7 ± 1.6	1.414 ± 0.012	400.0 ± 120.0	0.52 ± 0.08	−99	1750	5.2
IMW	17.1 ± 2.3	1.412 ± 0.009	890.0 ± 110.0	0.52 ± 0.06	−25	3980	12.0
HMW	36.6 ± 1.6	1.449 ± 0.009	2800.0 ± 280.0	0.77 ± 0.06	−424	7500	12.3
DEN	94.9 ± 9.5	1.439 ± 0.008	6700.0 ± 760.0	0.70 ± 0.05	−890	15800	7.3

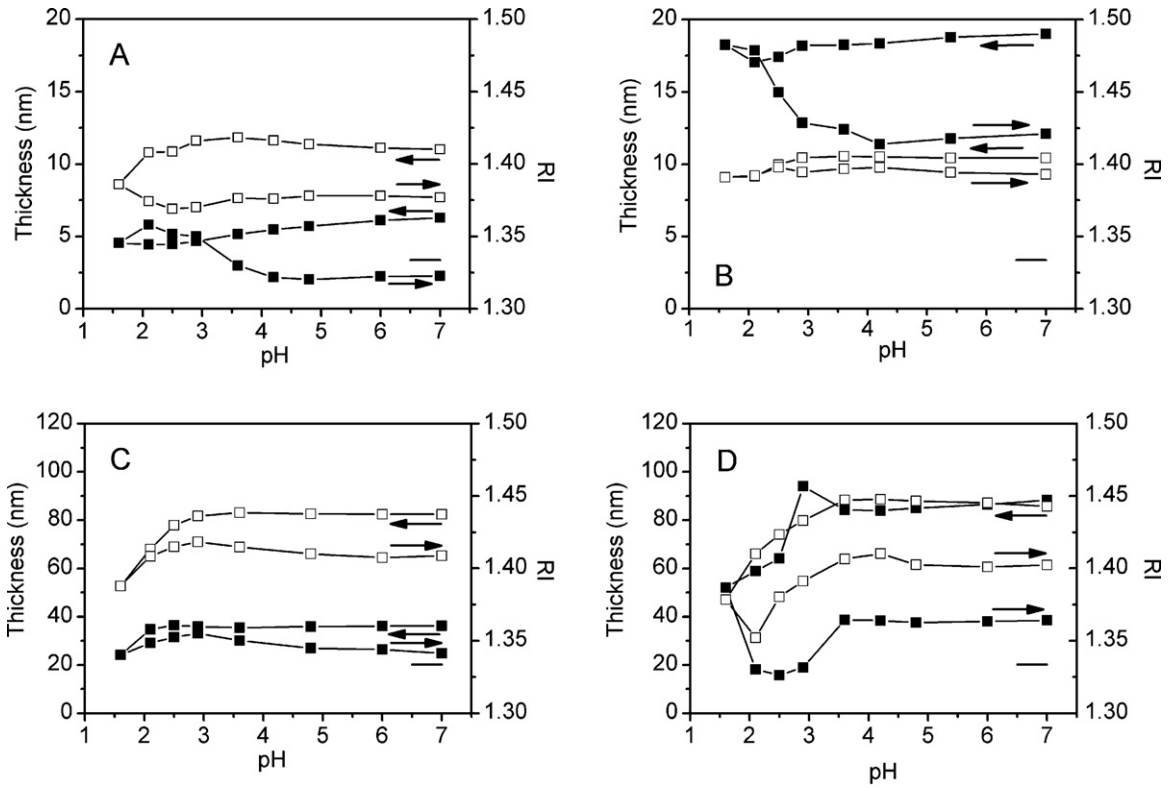

Fig. 2. Multilayer film pH-response measured *in situ* with DPI. 10 layer multilayers were assembled at pH 7.0. Optical thickness (■) and RI (□) are shown as a function of pH (14–16 steps). Key to PLLs: (A) LMW, (B) IMW, (C) HMW and (D) DEN. Horizontal bar denotes buffer RI of 1.3336.

DPI. Comparison of the dissipations allows the viscoelastic properties of the films to be compared. Voinova et al.'s model indicates that the dissipation of thin films is proportional to their thickness (Voinova et al., 1999; Westwood et al., 2010). For the multilayers assembled with the linear PLLs the HMW has a relatively low value considering its hydrated mass indicating that the PGalA-HMW PLL multilayers are relatively elastic. Similarly, the dissipation of the PGalA-DEN PLL is low despite its relatively large hydrated mass indicating relatively little viscous dissipation in the film and a predominantly "rigid elastic" response.

3.2. DPI characterisation of multilayer pH response.

The pH response of the four PGalA-PLL multilayers to a pH cycle ranging from pH 7.0 down to 1.6 and returning to 7.0 was followed using DPI. Fig. 2 shows the changes which occur in optical thickness and refractive index of the multilayer film as a function of pH.

In each case there is a reduction of both optical thickness and refractive index over the pH cycle. Using the De Feijter equation the refractive index can be converted to a polymer concentration using a typical refractive index increment, $dn/dc = 0.15\ \mathrm{mL\,g^{-1}}$. The refractive index of the buffer was assumed to be 1.3336. Combining the optical thickness and polymer concentration data allows the total polymer mass in the film to be estimated and these values are tabulated in Table 2. To aid interpretation the ratios of each quantity to its initial value are given in the table (in brackets to the right of each column). It can be observed that the pH challenge leads to an overall reduction in optical thickness in the range 33–73% and larger losses of polymer mass in the range 45–87% depending on the PLL used. Correspondingly the polymer concentrations of the final films are also reduced by between 20 and 50%. Overall it is the LMW PLL which shows the largest fractional loss of thickness and mass. The DEN PLL fractional losses are also significantly higher than those of the IMW and HMW PLLs. The LMW PLL also has the highest fractional loss of polymer concentration over the pH cycle whilst for the other PLLs this ratio falls within the range 0.74–0.80

The multilayers with the LMW and IMW PLL (Fig. 2A and B) show broadly similar behaviour in the response of the optical thickness to the pH challenge. There is relatively little change in optical thickness as the pH is reduced from 7.0 to 1.6. However, as the pH is increased the films thickness decreases in the pH range 2.0–4.5, then subsequently there is negligible change once the pH exceeds 4.5. The refractive index of the films, which reflects the polymer concentration, indicates significant decreases as the pH falls below 3.0. The polymer concentration of the LMW PLL multilayer continues to decrease until the pH is raised to 2.6. In comparison, the polymer concentration in the IMW PLL multilayer changes relatively little overall and remains essentially constant once the pH reaches 1.6.

The PGalA-HMW PLL multilayer shows reduced thickness and refractive index (polymer concentration) and corresponding loss of polymer mass (Table 2) as the pH is reduced below 3.0. At the lowest pH 1.6 the film reaches its minimum thickness and refractive index which corresponds to its lowest density. As the pH increases these changes are apparently reversed as the film is both increasing in thickness and density. This appears unphysical and it suggests that the total polymer mass in the multilayer film is increasing during the experiment whereas the polymer mass is expected to remain constant or decrease in a responsiveness experiment. This apparent anomaly is likely due to a changing heterogeneity of the film during the experiment. The final result after the pH challenge is a thinner, less dense film.

The PGalA-PLL dendrimer multilayer (Fig. 2D) shows the largest change in refractive index over the pH cycle. As the pH is reduced a small swelling event commences at pH 3.5 with simultaneous reduction of polymer concentration. As the pH is reduced there is a progressive decrease of thickness and density. As the pH is

Table 2
pH response of PGalA-PLL 10-layer multilayers characterised using DPI. The ratio of each quantity to its initial value is given in brackets.

PLL	pH[a]	Optical thickness (nm)	Polymer concentration (g mL^{-1})	Polymer mass (ng cm^{-2})
LMW	7.0i	6.4 ± 1 (1.0)	0.50 ± 0.02 (1.0)	320 ± 30 (1.0)
	1.6	4.7 ± 1 (0.73)	0.23 ± 0.10 (0.46)	170 ± 50 (0.34)
	7.0f	1.7 ± 1 (0.27)	0.25 ± 0.13 (0.50)	40 ± 25 (0.12)
IMW	7.0i	18.3 ± 1 (1.0)	0.51 ± 0.05 (1.0)	920 ± 100 (1.0)
	1.6	17.4 ± 1 (0.95)	0.39 ± 0.01 (0.77)	690 ± 100 (0.75)
	7.0f	11.9 ± 1 (0.65)	0.41 ± 0.02 (0.80)	500 ± 100 (0.54)
HMW	7.0i	36 ± 2 (1.0)	0.73 ± 0.06 (1.0)	2600 ± 200 (1.0)
	1.6	26 ± 2 (0.72)	0.44 ± 0.13 (0.60)	1200 ± 700 (0.46)
	7.0f	24 ± 8 (0.67)	0.54 ± 0.07 (0.74)	1300 ± 130 (0.50)
DEN	7.0i	95 ± 10 (1.0)	0.70 ± 0.05 (1.0)	6600 ± 760 (1.0)
	1.6	55 ± 5 (0.58)	0.29 ± 0.02 (0.41)	1600 ± 170 (0.24)
	7.0f	40 ± 14 (0.42)	0.54 ± 0.07 (0.77)	2100 ± 350 (0.32)

[a] i, initial; f, final.

then increased both thickness and refractive index pass through minima before restabilising at pH 4.8 as a thinner, less dense film.

To summarise, the LMW multilayers show the largest loss of polymer resulting in 50% loss of polymer concentration and 73% loss of thickness. The dendrimer shows an intermediate loss of mass resulting in a 23% loss of polymer concentration and a 58% loss of thickness. The IMW and HMW show lower losses of mass (45–50%) and while losses of thickness is the larger effect (33–35% loss), these are closer to the losses of concentration (20–26%). One feature of the HMW and DEN multilayers is an increase in refractive index as the pH is increased, the multilayer recovering its earlier density.

3.3. FTIR-ATR characterisation of multilayer pH response

The FTIR-ATR spectra provide information on the composition of the multilayers and the speciation of the carboxyl group of the PGalA throughout the pH cycle. Fig. 3 shows the spectra of the multilayers after assembly at pH 7.0, after the pH has been reduced to 1.6 and, finally, once the pH has been brought back to 7.0. The solid line is the FTIR spectra of the 10-layer multilayers as assembled at pH 7.0. The adsorption peak at 1606 cm^{-1} corresponds to the absorption due to the carboxylate group of the polygalacturonic acid. The amide I absorption overlaps with this and forms a shoulder in the region of 1643 cm^{-1}. Interestingly, although the dendrimer has a strong absorption peak at 1675 cm^{-1} in the solution state (results not shown), as part of a multilayer its predominant absorption appears at 1643 cm^{-1} (Fig. 3D), the common absorption frequency for randomly coiled polyamino acids and proteins (Dzwolak, Muraki, Kato, & Taniguchi, 2004; Fandrich & Dobson, 2002; Jackson, Haris, & Chapman, 1989; Shen, Chaudouet, Ji, & Picart, 2011). At pH 1.6 (dashed lines in Fig. 3) the spectra show the absorption bands of the anhydrogalacturonic acid residues (1732 cm^{-1}), the protonated form of the anhydrogalacturonate residues. In the solution state the pK_a of anhydrogalacturonic acid residues have a range of values less than 4.5 (Ralet et al., 2001)

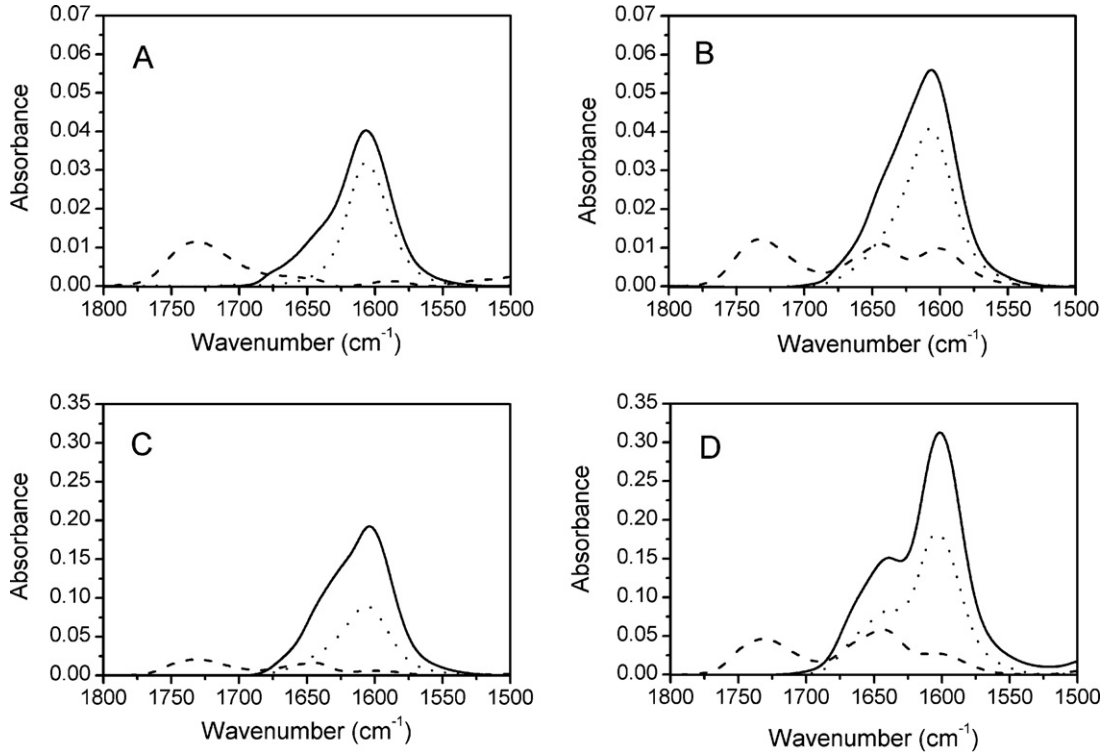

Fig. 3. FTIR spectra for pH-response of PGalA multilayers for PLLs: (A) LMW, (B) IMW, (C) HMW and (D) DEN. Solid line initial pH 7.0; dashed line pH 1.6; dotted line final pH 7.0.

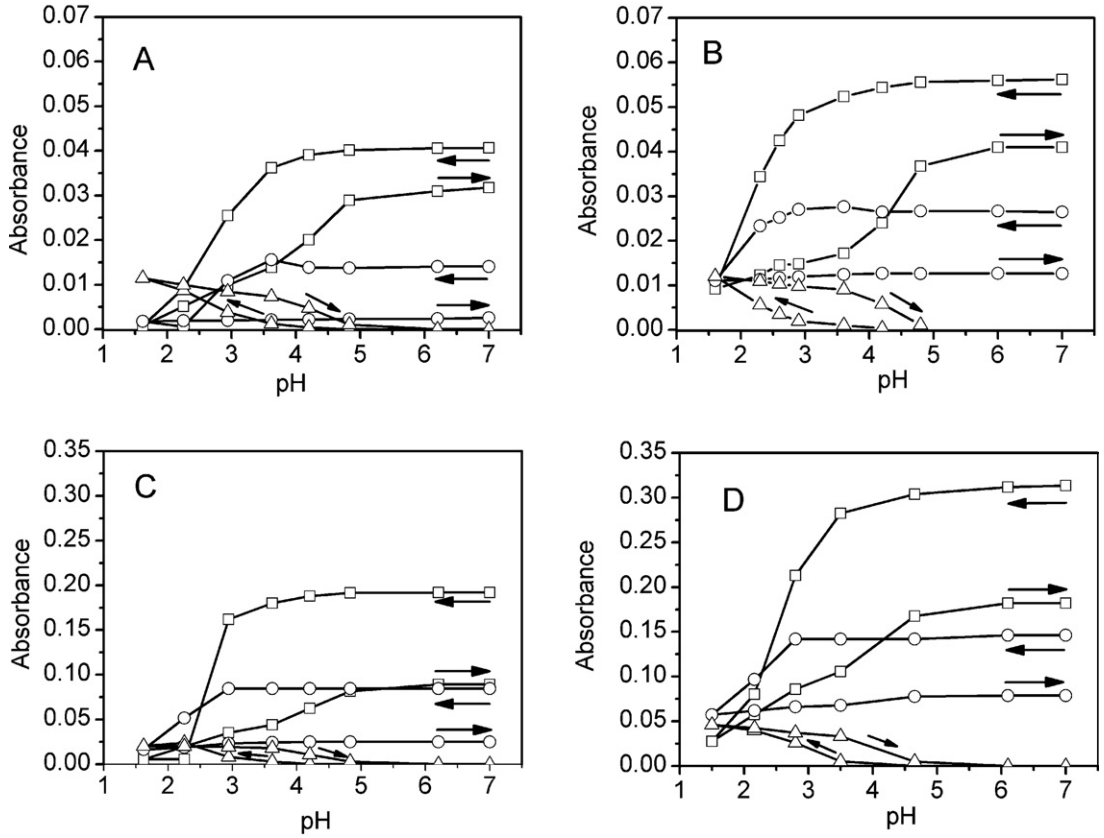

Fig. 4. Absorbance variation at 1606 cm^{-1} (carboxylate peak, squares), 1643 cm^{-1} (amide I, circles) and 1733 cm^{-1} (carboxylic COOH peak, triangles) as a function of pH for PGalA-PLL multilayers. PLL structures: (A) LMW, (B) IMW, (C) HMW and (D) DEN.

and so, over the acid cycle, the anhydrogalacturonate residues start from being fully ionised at pH 7.0 and, as the pH is reduced, bind protons which reaches a maximum at the lowest pH (1.6) and then, as the pH is increased to 7.0, the acidic groups ionise once again. We have previously shown that the predictions from solution state behaviour need to be refined since interactions within the deposited multilayer cause a shift in the apparent pK_a of about 2.0 units as the pH is reduced for the PGalA-IMW PLL multilayer (Westwood et al., 2011).

At pH 7.0 the spectra are dominated by the absorbance at 1606 cm^{-1} due to anhydrogalacturonate residues of the PGalA. The absorbance due to the amide I bands of the PLL overlap with that of PGalA and so, for the linear PLLs (Fig. 4A–C) they appear as a shoulder. The spectrum of the multilayer with the PLL dendrimer (Fig. 4D) does however shows a distinct peak in the amide I region.

Some qualitative conclusions can be drawn by comparing the shapes of the initial and final spectra at pH 7.0. Whereas the final spectrum of the PGalA-DEN PLL has a similar shape to the initial one, those for the linear PLLs particularly the LMW PLL show enhanced loss of absorbance at 1643 cm^{-1} indicative of the preferential loss of PLL over the pH cycle.

Fig. 4 shows the variation of the absorbance at 1606 cm^{-1}, 1643 cm^{-1} and 1733 cm^{-1} with pH which reveals more detail of the changing composition and speciation of the polymers within the multilayer. The absorbances and ratios to their initial values are shown in Table 3. Over the first half of the pH cycle the magnitude of the 1606 cm^{-1} peak falls to between 2 and 16% of its initial value largely due to the protonation of the anhydrogalacturonate residues. Over the second half of the cycle the absorbance increases once again as the groups ionise. The absorbance ratios show that as the molecular weight of the linear PLLs increase there are increasing losses of PGalA over the cycle which, neglecting the PLL absorbance at 1606 cm^{-1}, are estimated to increase from 22% to 54%. The variation of absorbance at 1643 cm^{-1} includes contributions from both the PLL and, to a lesser extent, PGalA–COO–. The contribution from PGalA at 1643 cm^{-1} is apparent in the second half of the pH cycle as an increase in absorbance which we assign to the increasing concentrations of anhydrogalacturonate residues.

However comparing the ratios describing decrease in absorbance over the pH cycle at 1606 cm^{-1} and 1643 cm^{-1} provides more detail on the preferential losses of PGalA and PLL over the cycle. The greatest preferential losses are for the LMW PLL and the lowest preferential losses are for the HMW PLL and DEN PLL.

Table 3
pH response of PGalA-PLL 10-layer multilayers characterised using FTIR-ATR absorbance. The value of the absorbance normalised to the initial value is in brackets.

PLL	pH[a]	1606 cm^{-1}	1643 cm^{-1}	1733 cm^{-1}
LMW	7.0i	0.041 (1.0)	0.014 (1.0)	0
	1.6	0.0008 (0.02)	0.0018 (0.13)	0.012
	7.0f	0.032 (0.78)	0.0026 (0.18)	0
IMW	7.0i	0.056 (1.0)	0.027 (1.0)	0
	1.6	0.0092 (0.16)	0.011 (0.42)	0.012
	7.0f	0.041 (0.73)	0.0126 (0.48)	0
HMW	7.0i	0.192 (1.0)	0.085 (1.0)	0
	1.6	0.0055 (0.03)	0.0164 (0.19)	0.020
	7.0f	0.089 (0.46)	0.0251 (0.30)	0
DEN	7.0i	0.314 (1.0)	0.146 (1.0)	0
	1.6	0.028 (0.09)	0.057 (0.39)	0.046
	7.0f	0.182 (0.58)	0.079 (0.54)	0

[a] i, initial; f, final.

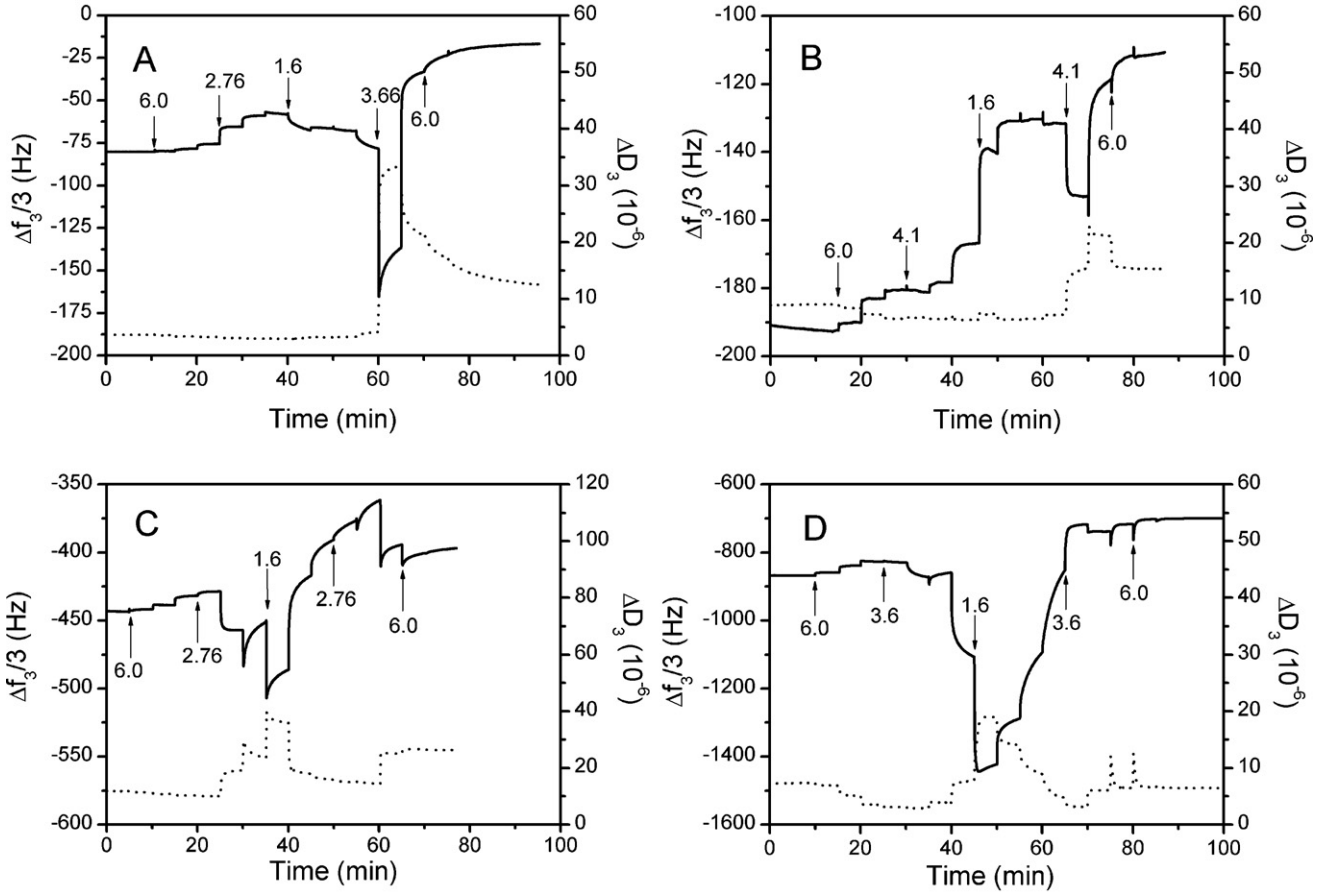

Fig. 5. QCMD frequency (solid line) and dissipation shifts (dashed line) in response to pH changes for PGalA-PLL multilayers. Key to PLLs: (A) LMW, (B) IMW, (C) HMW and (D) DEN.

The absorbance at 1733 cm^{-1} indicates the amount of PGalA which remains adsorbed at pH 1.6. This is quite similar for the LMW and IMW PLL-crosslinked multilayers and, approximately, doubles as the HMW PLL is used then doubles again as the DEN-PLL is used. However, the higher absorbances at 1733 cm^{-1} for the HMW and DEN PLL mulilayers are not in proportion to the initial absorbances at 1606 cm^{-1} indicating that these multilayers have lost more PGalA as the pH is reduced to 1.6.

3.4. QCMD measurements, hydrated mass and a consolidated description of multilayer response to pH

Fig. 5 shows the results of probing the pH responsiveness of the multilayer films using QCMD. The negative shift in frequency is interpreted as an increase in the hydrated mass of the film attached to the crystal oscillator.

The starting point of each frequency shift, $\Delta f_3/3$, corresponds to the 10 layer multilayer assembled in the first half of the experiment. The range of frequency shift on the ordinate has been selected to clearly show the features over the pH responsiveness experiment. Only the LMW PLL multilayer, Fig. 5A, experiment ends with a $\Delta f_3/3$ close to zero corresponding to very extensive desorption or detachment of the film from the sensor surface. The IMW PLL multilayer (Fig. 5B) falls to about 60% of its initial $\Delta f_3/3$ while the HMW and DEN PLL multilayers remain at about 80–90% of their initial values.

A common feature in all the experiments is a strong swelling–deswelling event. The pH onset of this event varies across the series occurring during pH increase in the second half of the experiment for the LMW PLL multilayer (pH 3.66) and IMW PLL multilayer (pH 4.1) and during the initial pH decrease for the HMW PLL (pH 2.4) and DEN PLL (pH 2.1). For the lower molecular weight PLLs (Fig. 5A and B) there is a sharp increase in $\Delta f_3/3$ and an equally sharp decrease, and for the HMW and DEN PLL the response occurs over a range of pH with a more gradual onset of the swelling and, similarly, gradual deswelling. It appears that the thinner films are rather fragile and brittle whereas the thicker films are less fragile and capable of a more plastic response.

Prior to this strong swelling–deswelling event, starting from pH 7.0, there is an initial decrease in the magnitude of $\Delta f_3/3$ corresponding to a decrease in hydrated mass. The DPI indicates some reduction of optical thickness (Table 2) and a larger reduction in polymer concentration as the pH is reduced. The FTIR-ATR indicates that greater amounts of PLL are being lost as compared with PGalA (Fig. 3). This is occurring as the PGalA is binding protons and so charge interactions between PGalA and PLL will be weakening. At low pH, PGalA can self associate which favours its retention in the multilayer and the preferential loss of the PLL (Alonso-Mougan, Fraga, Meijide, Rodriguez-Nunez & Vazquez-Tato, 2003).

As the pH increases the PGalA ionises. In previous work (Westwood et al., 2011) we have shown there is a hysteresis effect. When the multilayer is assembled the interactions cause the protonation of the galacturonic acid residues to be shifted about 2 pH units down the pH scale. Once the mixture has been cycled through low pH these interactions are lost and the ionisation, as the pH increases, is closer to that expected for dilute solution pK_a's (Ralet et al., 2001). The PGalA ionisation is apparent in the FTIR-ATR (Fig. 4) and is essentially complete by pH 5.0. In the HMW PLL and DEN PLL multilayer the QCMD shows (Fig. 5C and D) large swelling events at pH 1.6 which subside as the pH increases and the PGalA ionises. Any PGalA self-association would be broken and

PGalA-PLL charge interactions could be re-established. This is consistent with deswelling occurring as these interactions are re-established which, after the loss of a proportion of the polymers and the intimate interactions created during layer-by-layer deposition, results in a thinner, less dense layer.

There is no obvious analogue of the sharp swelling–deswelling event observed for the LMW and IMW PLL in the QCMD (Fig. 5A and B) in the DPI results (Fig. 2A and B). The FTIR-ATR (Fig. 4A and B) shows that the event occurs as the charge on the PGalA is increasing rapidly. The re-structuring within the multilayer appears to result in some marked change in material properties which is apparent in the acoustic measurements (QCMD) though goes undetected in optical measurements (DPI).

4. Conclusions

This study characterises the effect of cationic crosslinker (PLL) structure on growth and pH responsiveness of PGaLA-based multilayers. Both the molecular weight of linear PLL and the branched structure of a dendrimer were found to affect multilayer growth and pH response.

The structural and compositional changes in response to a neutral to acid to neutral pH cycle occurred at pH below 5.0, corresponding to conditions at which the PGaLA binds protons on pH decrease and ionises on pH increase. The LMW PLL crosslinker yielded a thin multilayer which preferentially lost crosslinker during the pH challenge and resulted in an even thinner vestigial mixed adsorbed layer. The effect of increasing the molecular weight to a HMW PLL crosslinker was to yield a thicker denser multilayer which, on acid pH challenge, lost 50–65% of its polymers leaving a residual film at the end of the challenge. The dendrimer was an effective crosslinker resulting in the thickest multilayer studied with a pH response similar to the HMW crosslinked PLL multilayer.

Overall variation of polycationic crosslinker molecular weight and branching offers a means of modifying multilayer pH responsiveness whilst maintaining some of the characteristics of the polyanion. For gastrointestinal applications pH variation is an important facet of the changing environment on passing down the GI tract. However, it is also possible to exploit the changing hydrolytic environment determined by the digestive enzymes. Future work will determine multilayer response to the combined effects of pH and, through suitable choice of polymers, hydrolytic enzymes.

Acknowledgements

The UK Biotechnology and Biological Sciences Research Council supported this research from the Institute Strategic Grant of the Institute of Food Research, Norwich, and through the award of the responsive mode grants (BBE0131711 and BBE0110041). The authors also wish to thank Dr. Nikolaus Wellner for his support.

References

Alberts, B., Johnson, A., Lewis, J., Raff, M., Roberts, K., & Walter, P. (2002). *Molecular biology of the cell*. New York: Taylor & Francis.

Alonso-Mougan, M., Fraga, F., Meijide, F., Rodriguez-Nunez, E., & Vazquez-Tato, J. (2003). Aggregation behaviour of polygalacturonic acid in aqueous solution. *Carbohydrate Polymers*, *51*(1), 37–45.

Bosman, A. W., Janssen, H. M., & Meijer, E. W. (1999). About dendrimers: Structure, physical properties, and applications. *Chemical Reviews*, *99*(7), 1665–1688.

Boudou, T., Crouzier, T., Ren, K. F., Blin, G., & Picart, C. (2010). Multiple functionalities of polyelectrolyte multilayer films: New biomedical applications. *Advanced Materials*, *22*(4), 441–467.

Boulmedais, F., Bozonnet, M., Schwinte, P., Voegel, J. C., & Schaaf, P. (2003). Multilayered polypeptide films: Secondary structures and effect of various stresses. *Langmuir*, *19*(23), 9873–9882.

Burke, S. E., & Barrett, C. J. (2003). pH-responsive properties of multilayered poly(L-lysine)/hyaluronic acid surfaces. *Biomacromolecules*, *4*(6), 1773–1783.

Burke, S. E., & Barrett, C. J. (2004). pH-dependent loading and release behavior of small hydrophilic molecules in weak polyelectrolyte multilayer films. *Macromolecules*, *37*(14), 5375–5384.

Cottet, H., Martin, M., Papillaud, A., Souaid, E., Collet, H., & Commeyras, A. (2007). Determination of dendrigraft poly-L-lysine diffusion coefficients by Taylor dispersion analysis. *Biomacromolecules*, *8*, 3235–3243.

Cros, S., Garnier, C., Axelos, M. A. V., Imberty, A., & Perez, S. (1996). Solution conformations of pectin polysaccharides: Determination of chain characteristics by small angle neutron scattering, viscometry, and molecular modeling. *Biopolymers*, *39*(3), 339–352.

Crouzier, T., Boudou, T., & Picart, C. (2010). Polysaccharide-based polyelectrolyte multilayers. *Current Opinion in Colloid & Interface Science*, *15*(6), 417–426.

Crouzier, T., & Picart, C. (2009). Ion pairing and hydration in polyelectrolyte multilayer films containing polysaccharides. *Biomacromolecules*, *10*(2), 433–442.

De Feijter, J. A., Benjamins, J., & Veer, F. A. (1978). Ellipsometry as a tool to study adsorption behavior of synthetic and biopolymers at air–water interface. *Biopolymers*, *17*(7), 1759–1772.

Decher, G. (1997). Fuzzy nanoassemblies: Toward layered polymeric multicomposites. *Science*, *277*(5330), 1232–1237.

Dzwolak, W., Muraki, T., Kato, M., & Taniguchi, Y. (2004). Chain-length dependence of alpha-helix to beta-sheet transition in polylysine: Model of protein aggregation studied by temperature-tuned FTIR spectroscopy. *Biopolymers*, *73*(4), 463–469.

Fandrich, M., & Dobson, C. M. (2002). The behaviour of polyamino acids reveals an inverse side chain effect in amyloid structure formation. *EMBO Journal*, *21*(21), 5682–5690.

Girod, S., Boissere, M., Longchambon, K., Begu, S., Tourne-Petheil, C., & Devoisselle, J. M. (2004). Polyelectrolyte complex formation between iota-carrageenan and poly(L-lysine) in dilute aqueous solutions: A spectroscopic and conformational study. *Carbohydrate Polymers*, *55*(1), 37–45.

Guzey, D., & McClements, D. J. (2006). Formation, stability and properties of multilayer emulsions for application in the food industry. *Advances in Colloid and Interface Science*, *128*, 227–248.

Halthur, T. J., Claesson, P. M., & Elofsson, U. M. (2006). Immobilization of enamel matrix derivate protein onto polypeptide multilayers. Comparative in situ measurements using ellipsometry, quartz crystal microbalance with dissipation, and dual-polarization interferometry. *Langmuir*, *22*(26), 11065–11071.

Hiller, J., & Rubner, M. F. (2003). Reversible molecular memory and pH-switchable swelling transitions in polyelectrolyte multilayers. *Macromolecules*, *36*(11), 4078–4083.

Hook, F., Kasemo, B., Nylander, T., Fant, C., Sott, K., & Elwing, H. (2001). Variations in coupled water, viscoelastic properties, and film thickness of a Mefp-1 protein film during adsorption and cross-linking: A quartz crystal microbalance with dissipation monitoring, ellipsometry, and surface plasmon resonance study. *Analytical Chemistry*, *73*(24), 5796–5804.

Jackson, M., Haris, P. I., & Chapman, D. (1989). Conformational transitions in poly(L-lysine)—studies using Fourier-transform infrared-spectroscopy. *Biochimica et Biophysica Acta*, *998*(1), 75–79.

Krzeminski, A., Marudova, M., Moffat, J., Noel, T. R., Parker, R., Wellner, N., et al. (2006). Deposition of pectin/poly-L-lysine multilayers with pectins of varying degrees of esterification. *Biomacromolecules*, *7*(2), 498–506.

Kujawa, P., Moraille, P., Sanchez, J., Badia, A., & Winnik, F. M. (2005). Effect of molecular weight on the exponential growth and morphology of hyaluronan/chitosan multilayers: A surface plasmon resonance spectroscopy and atomic force microscopy investigation. *Journal of the American Chemical Society*, *127*(25), 9224–9234.

Li, X., & Jasti, B. R. (Eds.). (2006). *Design of controlled release drug delivery systems*. New York: McGraw-Hill.

Li, Y., Hu, M., Xiao, H., Du, Y. M., Decker, E. A., & McClements, D. J. (2010). Controlling the functional performance of emulsion-based delivery systems using multi-component biopolymer coatings. *European Journal of Pharmaceutics and Biopharmaceutics*, *76*(1), 38–47.

Lu, J. R., Swann, M. J., Peel, L. L., & Freeman, N. J. (2004). Lysozyme adsorption studies at the silica/water interface using dual polarization interferometry. *Langmuir*, *20*(5), 1827–1832.

McClements, D. J., & Li, Y. (2010). Structured emulsion-based delivery systems: Controlling the digestion and release of lipophilic food components. *Advances in Colloid and Interface Science*, *159*(2), 213–228.

Moffat, J., Noel, T. R., Parker, R., Wellner, N., & Ring, S. G. (2007). The environmental response and stability of pectin and poly-L-lysine multilayers. *Carbohydrate Polymers*, *70*, 422–429.

Ono, S. S., & Decher, G. (2006). Preparation of ultrathin self-standing polyelectrolyte multilayer membranes at physiological conditions using pH-responsive film segments as sacrificial layers. *Nano Letters*, *6*(4), 592–598.

Pommersheim, R., Schrezenmeir, J., & Vogt, W. (1994). Immobilization of enzymes by multilayer microcapsules. *Macromolecular Chemistry and Physics*, *195*(5), 1557–1567.

Porcel, C., Lavalle, P., Decher, G., Senger, B., Voegel, J. C., & Schaaf, P. (2007). Influence of the polyelectrolyte molecular weight on exponentially growing multilayer films in the linear regime. *Langmuir*, *23*(4), 1898–1904.

Ralet, M. C., Dronnet, V., Buchholt, H. C., & Thibault, J. F. (2001). Enzymatically and chemically de-esterified lime pectins: Characterisation, polyelectrolyte behaviour and calcium binding properties. *Carbohydrate Research*, *336*(2), 117–125.

Sauerbrey, G. (1959). Verwendung von Schwingquarzen zur Wägung dünner Schichten und zur Mikrowägung. *Zeitschrift für physik*, *155*(2), 206–222.

Shen, L. Y., Chaudouet, P., Ji, J. A., & Picart, C. (2011). pH-amplified multilayer films based on hyaluronan: Influence of HA molecular weight and concentration on film growth and stability. *Biomacromolecules*, *12*(4), 1322–1331.

Sukhorukov, G. B., & Mohwald, H. (2007). Multifunctional cargo systems for biotechnology. *Trends in Biotechnology*, *25*(3), 93–98.

Voinova, M. V., Rodahl, M., Jonson, M., & Kasemo, B. (1999). Viscoelastic acoustic response of layered polymer films at fluid–solid interfaces: Continuum mechanics approach. *Physica Scripta*, *59*(5), 391–396.

Wen, Y. P., & Dubin, P. L. (1997). Potentiometric studies of the interaction of bovine serum albumin and poly(dimethyldiallylammonium chloride). *Macromolecules*, *30*(25), 7856–7861.

Westwood, M., Noel, T. R., & Parker, R. (2010). The characterisation of polygalacturonic acid-based layer-by-layer deposited films using a quartz crystal microbalance with dissipation monitoring, a dual polarization interferometer and a Fourier-transform infrared spectrometer in attenuated total reflectance mode. *Soft Matter*, *6*(21), 5502–5513.

Westwood, M., Noel, T. R., & Parker, R. (2011). Environmental responsiveness of polygalacturonic acid-based multilayers to variation of pH. *Biomacromolecules*, *12*(2), 359–369.

Zhi, Z. L., & Haynie, D. T. (2004). Direct evidence of controlled structure reorganization in a nanoorganized polypeptide multilayer thin film. *Macromolecules*, *37*(23), 8668–8675.